Analyses of 1-min Rain Rates Extracted from Weighing Raingage Recordings

PAUL TATTELMAN

Air Force Geophysics Laboratory, Hanscom AFB, Massachusetts

RICHARD W. KNIGHT

National Climatic Data Center, Asheville, North Carolina

(Manuscript received 25 September 1987, in final form 8 January 1988)

ABSTRACT

A method for extracting 1-min rain rates from original weighing raingage recordings is described. The method allows the retrieval of rates for long periods at approximately 300 United States weather stations. The process combines magnification of original chart records with modern digitizing and filtering techniques to obtain the 1-min data that are ordinarily unreadable. Analyses are presented of the frequency and duration of 1-min rates for these seven locations and an eighth location, for which data were collected using a high speed recorder.

1. Introduction

Rain is a major design consideration for equipment that must operate in or through the troposphere. In addition to the mechanical impact of rain (e.g., erosion on the leading edges of aerospace vehicles, leakage into sealed components, etc.), it is a major cause of attenuation of microwave signals used in communications. Satellite communication systems employing EHF (extremely high frequency) are especially vulnerable to attenuation due to rain.

One-min rainfall rates are generally considered most practical for design considerations and as input to attenuation models. Records of rainfall amounts for periods less than 1 h are not readily available, however. Amounts for increments less than 5-min were primarily collected during special field programs for limited time periods, generally 1 to 3 yr. This has prompted the development of numerous models to estimate frequencies of 1-min rates (Tattelman and Grantham 1985).

For most mechanical design considerations involving rain, it is sufficient to know probabilities of extreme rates at locations noted for heavy rain (Tattelman and Willis 1985). Attenuation of radio signals can be significant, however, at relatively low rain rates that occur with varying probabilities just about anywhere in the world. Therefore, statistics on the frequency and duration of 1-min rain rates are required for locations representing many climatic rainfall regimes (Tattelman and Scharr 1983). These can be used in attenuation models to determine required power levels, the frequency and duration of communication outages, and the need for space diversity of terminals or other alternatives. This article describes a method used for extracting 1-min rates from a largely untapped reservoir of original raingage recordings, and presents analyses of the data obtained for eight locations.

2. Data

Weighing raingage recordings for approximately 300 first-order United States weather stations are archived on microfiche at the National Climatic Data Center (NCDC), Asheville, North Carolina. Ten years of 1-min rain rate data for eight locations were analyzed for this study; rain rates for solid precipitation represent melted values. The locations, the percent of time it rained at each location, and the percent of the rain data that was missing over the 10 yr is provided in Table 1.

Missing data represent periods of rain when chart records were unavailable for digitizing. Hourly totals were available, however, so it was possible to estimate the percent of total rain data that was missing at each location. This was done by dividing the clock hours of rain for which chart records were not available by the total number of clock hours of rain at each location. For this calculation, a clock hour of rain is a 60-min interval, starting on the hour, in which a measurable amount of rain has fallen.

The data at all locations except Urbana, Illinois were obtained from raingage recordings stored at NCDC for the period 1 January 1970–31 December 1979. As part

Corresponding author address: Mr. Paul Tattelman, AFGL/LYA, Hanscom AFB, MA 01731.

TABLE 1. Locations for which 10 yr of 1-min rain rate data were studied. The percent of time it rains, and the estimated percent of the rain data that are missing is provided.

Location	Elevation (m)	Time it rains (%)					Estimated rain data missing (%)
		Jan	Apr	Jul	Oct	Annual	
Boston, Mass.	5	8.7	6.6	3.1	5.4	6.3	2.0
Denver, Colo.	1610	1.7	4.6	1.9	2.6	2.8	2.7
Grand Junction, Colo.	1475	2.8	2.1	0.8	2.2	1.8	2.6
Key West, Fla.	3	1.8	1.0	2.6	2.8	2.3	3.7
Omaha, Nebr.	300	2.8	5.4	2.8	4.2	3.7	13.3
Rapid City, S. Dak.	965	2.1	5.8	2.6	2.6	3.0	6.6
Seattle, Wash.	120	14.0	6.5	2.3	7.3	8.1	2.4
Urbana, Ill.	175	4.7	4.1	2.7	3.6	4.1	1.2*

* This value represents percent of full operational time.

of this study, a weighing raingage was checked for its mechanical response time. The response time, once the water was in the weighing bucket, was a fraction of a second. The funnel channeling the water into the bucket allowed a flow of water equivalent to a rainfall rate of approximately 84 mm min^{-1}, well in excess of the world record 1-min accumulation of 31 mm (Engelbrecht and Brancato 1959). Thus, the total raingage response for the world-record rate is a small fraction of a minute. The 1-min record itself was determined from a weighing raingage chart.

The data for Urbana were obtained from the Illinois State Water Survey, Champaign, Illinois as part of a USAF contract (Jones and Wendland 1983, 1984). The Urbana data cover a period of 10.25 yr from 1 June 1969 to 31 August 1979. They were obtained using a high-speed weighing raingage recorder described in the references. The original Urbana data were used without modification.

3. Extraction of 1-min rates

The trace on a weighing raingage chart (Fig. 1) is the representation of the integral of the rainfall rate over time. To obtain rates, we differentiate the function which describes the trace at each point of interest, i.e., at each minute. The rate is equal to the slope of the tangent to the curve at each 1-min interval. In actual practice, the slope is obtained by taking differences along the trace. Differentiation by this method can be

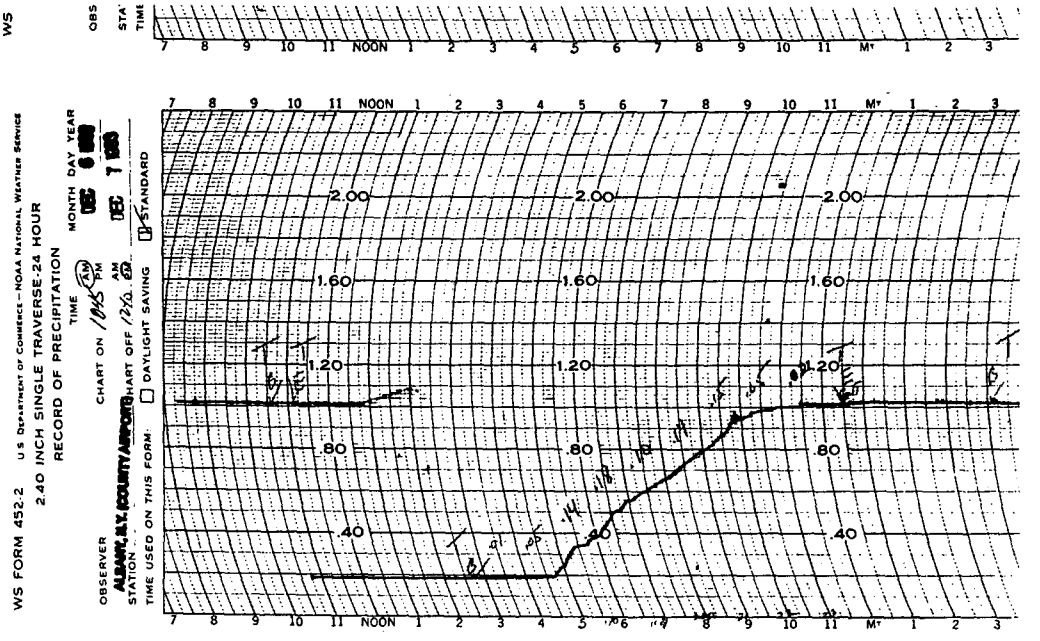

FIG. 1. Standard weighing raingage trace (smaller than original).

a very noisy process, however, even when the errors in measurement are quite small. The reason is that the computed slope is very sensitive to small changes in x and y coordinates, especially along the steeper portions of the trace.

A digitized trace, whether digitized by an automated curve follower or manually by a technician, tends to wander back and forth about the recorded trace. As a result, a time series of derived rainfall rates will contain a high frequency noise component whose amplitude tends to increase with increasing rates. Therefore, the high rates which we are most interested in are likely to have the largest errors. The process of eliminating these errors is described in two articles by Ruthroff and Bodtmann (1976) and Bodtmann and Ruthroff (1976).

a. Digitization

Hourly rainfall amounts for all United States first-order weather stations are published monthly by NCDC in *Local Climatological Data.* This publication was used to determine periods of measurable rain at selected stations. Paper copies of the microfiche records for these periods were enlarged to more than twice their original size. This was done with care and checks of the chart grid to avoid any distortion. The original chart has a resolution of 0.2 mm min^{-1} (e.g., a 15-min time interval is 3 mm long). Our trial tests showed that we could consistently digitize points with a repeatability of ± 0.1 mm which corresponds to ± 0.5 min on original size charts. By expanding the charts to a resolution of 0.428 mm min^{-1} we have essentially halved the uncertainty in the time-axis measurements to one-quarter minute.

The precipitation traces are digitized manually by following the trace with a cursor. The digitizer is an electronic device that records the x–y coordinates that are transmitted by the cursor. Each precipitation trace is sampled using the incremental stream mode of the digitizing tablet. This means that a point is recorded each time the cursor is moved a prescribed distance along the trace, which in this application is set at 0.25 mm. Therefore, during low rainfall rate episodes (flat trace) points are sampled at approximately 1-half min intervals. During high-rate episodes (sharp curve) the points are sampled at smaller intervals of time, thus the sampling rate per minute is higher.

b. Processing

For the reasons discussed earlier, we know that the computations of rainfall rates will be contaminated by a high-frequency noise component induced by small inaccuracies in the digitized representation of the trace. Our goal is to remove the noise and recover the signal. This is done by employing a suitable low-pass filter.

The computational steps employed in our 1-min rain rate processing were based on the procedures in Ruthroff and Bodtmann (1976). They are

- One-half minute interpolation. Linear interpolation is used to produce both an x- and a y-coordinate value for each ½-min increment of the precipitation episode. Digitizing errors occur with equal likelihood in x and y. The interpolation procedure, however, forces all of the error onto the y coordinate only, which simplifies subsequent processing.
- Running mean smoother. A three-point running mean smoother is applied to the ½-min data to ameliorate the effects of some of the larger inconsistencies.
- Detrend trace. This allows the data representing the precipitation trace to be expanded into a finite Fourier series.
- Fourier expansion. The detrended data are converted from the time domain into the frequency domain by use of a fast Fourier transform (FFT).
- Fourier filter. Filtering is accomplished by disregarding all of the Fourier coefficients which fall beyond the filter cutoff and then reconstructing the precipitation trace with the coefficients that remain.
- Final smoother. A cubic spline smoother is invoked to eliminate residual sinusoidal components resulting from the filter.
- Rate computation. The filtered trace is made monotonically increasing to eliminate negative rainfall rates. One-minute rates are computed and those less than 0.25 mm h^{-1} are set to zero.

1) FILTERING AND SMOOTHING

(i) *Fourier expansion.* Any stationary time series can be transformed from the time domain to the frequency domain by the following (Bloomfield 1976):

$$X_t = A_0 + \sum (A_j \cos\omega_j t + B_j \sin\omega_j t), \quad 0 < j \leq n/2 \tag{1}$$

where X_t represents values at time t, A_0 is the mean of the time series, ω the Fourier frequency, and A_j and B_j are coefficients. Each point X_t of the function is calculated by summing sines and cosines of each of the j Fourier frequencies and weighting each by a Fourier coefficient (A_j, B_j). The Fourier frequencies ω_j can have the dimension of cycles per unit of time ($\omega_j = 2\pi j/n$) where n is the number of data points. Since it takes a minimum of two points to represent the shortest cycle, there can be a maximum of $n/2$ Fourier frequencies. In this application, we have data values equally spaced at ½-min intervals. Therefore, a precipitation episode lasting, say, 2 h, will have 240 points. (Episodes range from 1 to 8 h for our filtering process.) The highest resolvable frequency will be at $j = 240/2 = 120$ and will have a value of $\omega_j = 120/240 = 0.5$ cycles per ½ min or 1 cycle/min^{-1}. The lowest frequency, of course, is always 1 cycle per total period, which in this example corresponds to a wavelength of 2 h. Thus, a Fourier decomposition of our 2-h episode consists of waves having periods from 1 min to 2 h.

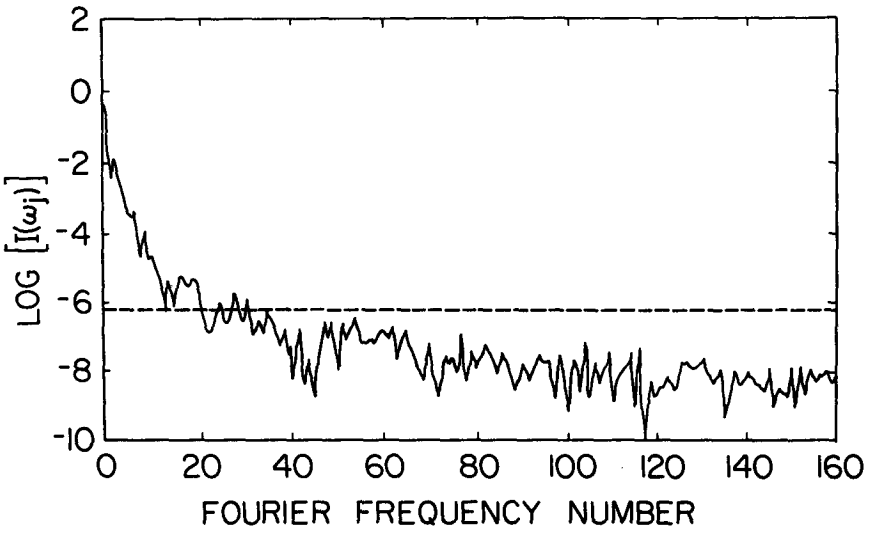

FIG. 2. Example of a periodogram used to determine Fourier frequency cutoff.

The fact that a digitized precipitation trace can be represented as a combination of contributions from many wavelengths makes the Fourier transform attractive as a filtering tool. We now have a means to separate the contributions supplied by the short wavelength noise from the longer wavelength contributions associated with the real precipitation episode.

(ii) *Fourier filter.* The Fourier expansion of the detrended precipitation trace yields $n/2$ Fourier coefficients. Low-pass rectangular filtering is accomplished by setting to zero all of the A_j and B_j coefficients beyond the j that is chosen as the filter cutoff. The obvious question is, Where does one place the filter cutoff?

To obtain insight into which frequencies contribute most to the signal, we compute the following function:

$$I(\omega_j) = \frac{n}{8\pi}(A_j^2 + B_j^2) \quad \text{for} \quad j = 1, 2, \cdots n, \quad (2)$$

where n is the number of ½-min intervals and A_j and B_j are coefficients in Eq. 1. The plot of $\log[I(\omega_j)]$ vs j, known as the periodogram (Bloomfield 1976) is used because the variation between frequencies is generally several orders of magnitude. The signal spectrum will decrease rapidly to a flatter, randomly oscillating spectrum resulting from noise. The filter cutoff should be

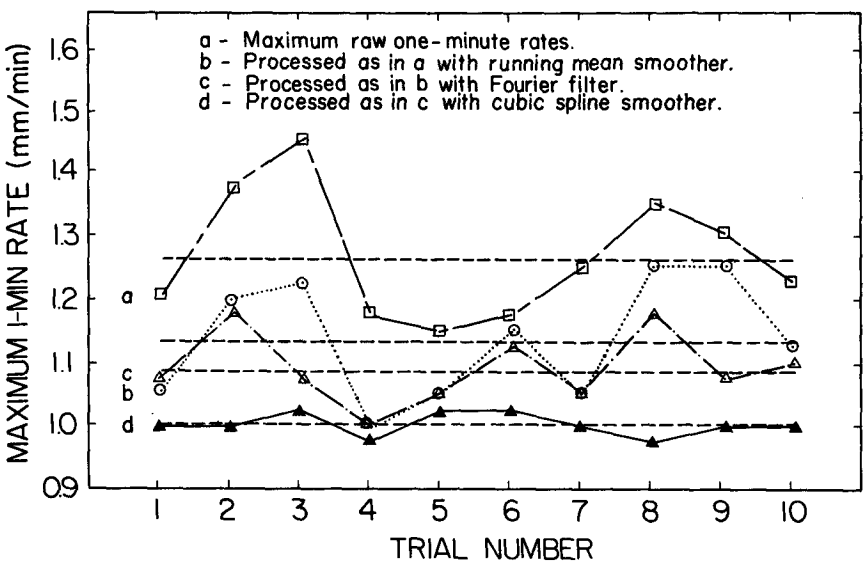

FIG. 3. Effects of various processing steps on the computed maximum 1-min precipitation rate.

placed at the intersection where the steep portion of the curve meets the flatter one. An example of a periodogram with the filter cutoff represented by a dashed line is shown in Fig. 2.

(iii) *Cubic spline smoother.* When the precipitation trace is reconstructed without the shorter wavelengths associated with noise, the filtered trace may display a very subtle sinusoidal oscillation. This, of course, is an artifact resulting from the sine–cosine basis used in the Fourier decomposition. While the total effect upon the rate computations is small, it does give a time series of computed rates a rather unnatural appearance. Therefore, a cubic spline smoothing routine with a variable sensitivity parameter is used to mitigate the oscillation.

2) TUNING FOR OBJECTIVE ANALYSIS

Section 3b1 explains the method for selection of the filter cutoff parameter. Visual inspection of the periodogram for each of the thousands of precipitation episodes that are being processed is clearly impractical, however. Therefore, an automated parameter selection criterion optimized for high precipitation rates was instituted.

Two simulated precipitation episodes were used to determine the characteristic noise structure associated with manually digitizing high-rate precipitation. Each trace was digitized ten times by the same person. As expected, the rate computations were quite noisy and there was a rather large variability in the value for the maximum 1-min rate. Figure 3 shows the effects of

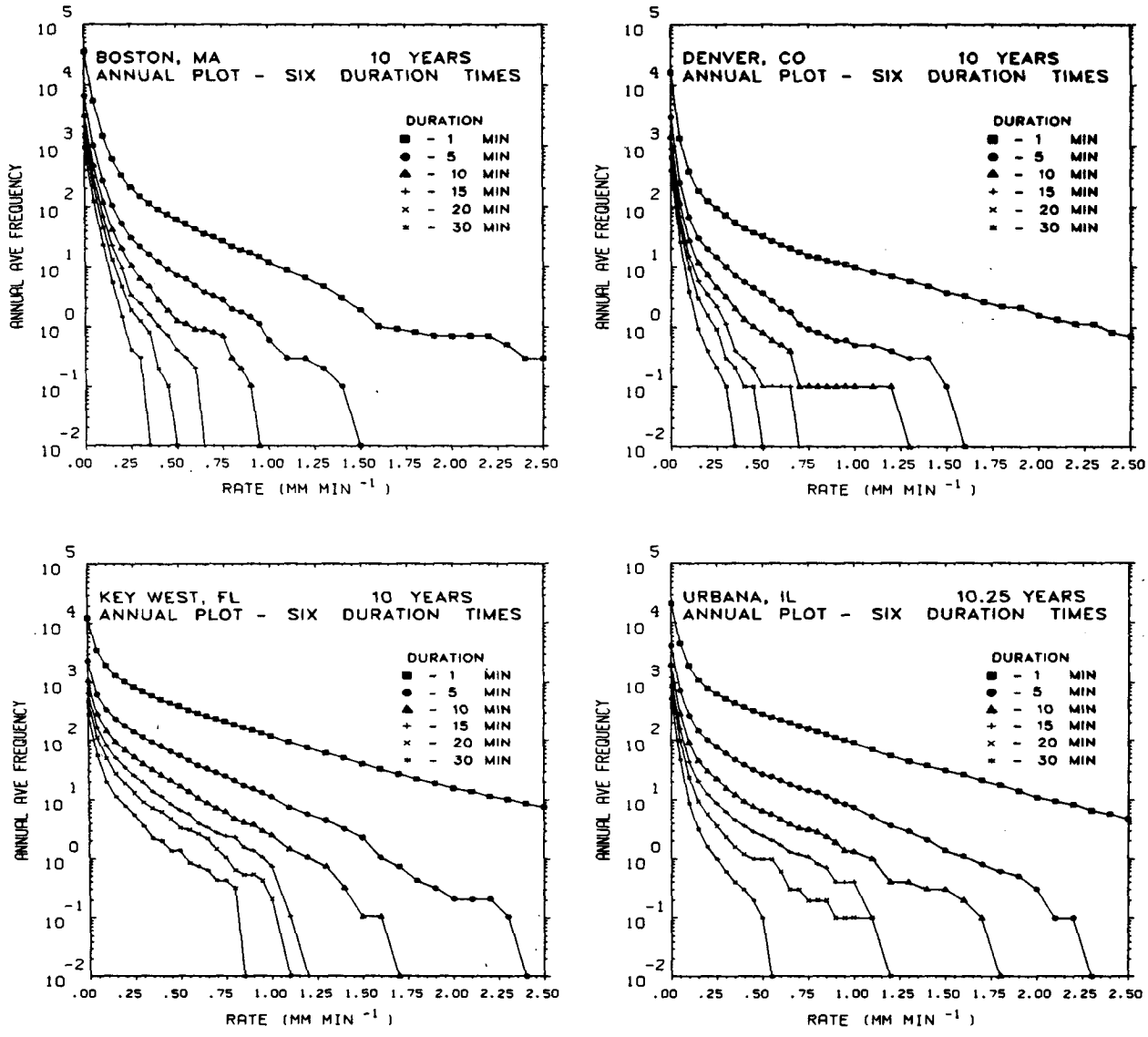

FIG. 4. Average annual frequency of 1-min rain rates for six duration times at Boston, Denver, Key West, and Urbana.

various processing steps on the magnitude of the maximum 1-min rate for one of the episodes. The uncorrected mean was 1.27 mm min^{-1}. When all of the processing steps were used (curve d in Fig. 3), the values for the maximum rate stabilized around the corrected value of 1 mm min^{-1}.

Based on these two sets of trials, cutoff parameters were chosen which were a function of the length of the precipitation episode, which, for our filtering process, ranged from 1 to 8 h. The value of the parameter begins at −5.5 for a 1-h event and decreases in increments of 0.1 for each additional hour in the time series. The cutoff selection criteria were validated by many experiments using actual digitized data and various analytic functions.

Normally, a single pass will be made through the filtering and smoothing routines, however, a check is made to determine the maximum 1-min difference in rate between the filtered and unfiltered data. This is done to ensure that the filter has not excessively smoothed a high-rate precipitation event. If the maximum difference exceeds 0.25 mm min^{-1}, an additional filter iteration is invoked. The filter cutoff parameter is decreased by 0.1 and new rates are computed. This process continues, if necessary, for a maximum of three iterations.

As a final check, the experiment conducted in Ruthroff and Bodtmann (1976) was repeated. In that experiment, white noise was added to the function

$$y = 1 - \exp(-2x^3)$$

and rates were computed before and after filtering. The

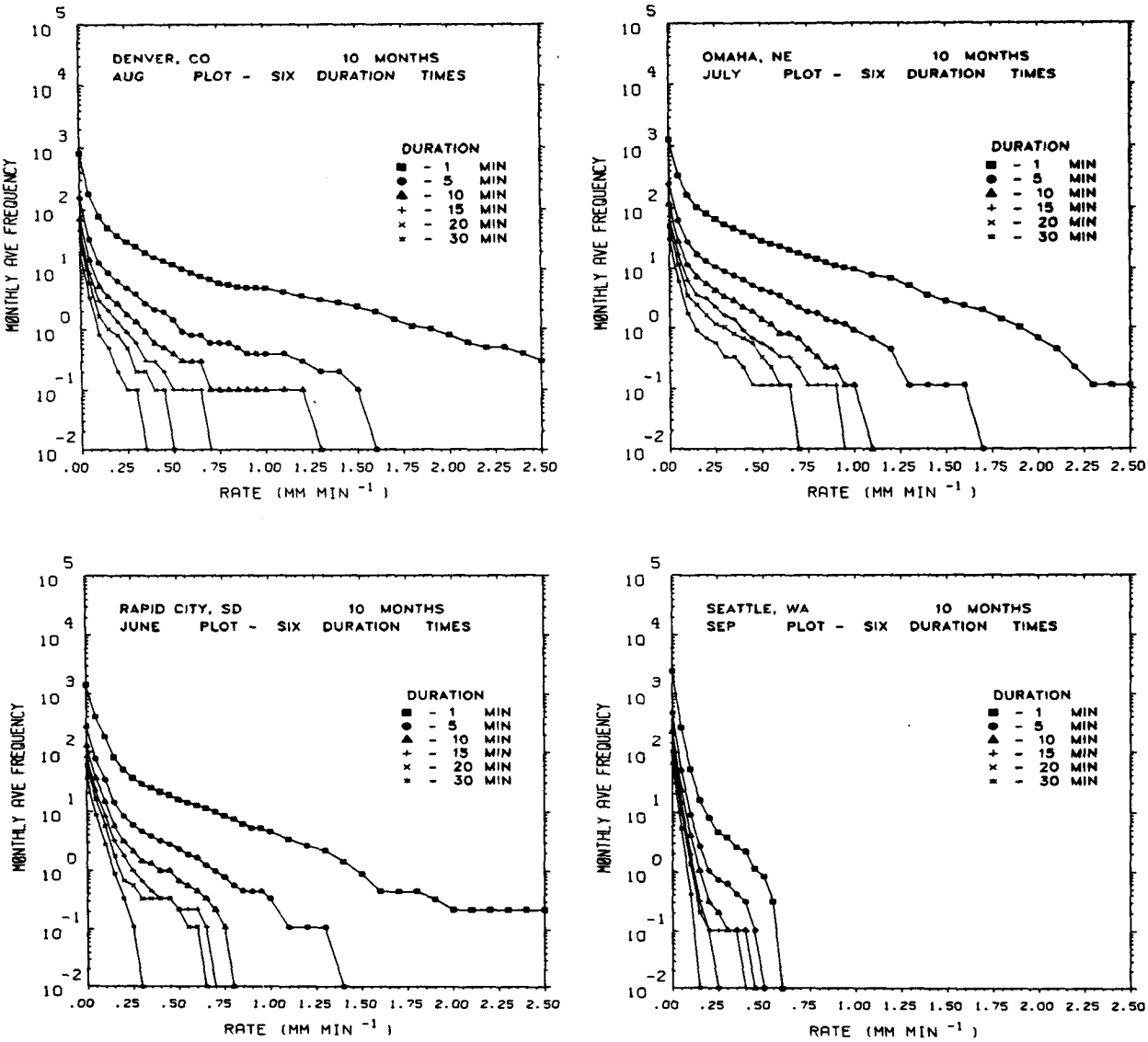

FIG. 5. Average worst-month frequency of 1-min rain rates for six duration times at Denver, Omaha, Rapid City and Seattle.

filter was able to recover the original signal with a high degree of accuracy. Our processing steps were also very successful in recovering the original signal.

c. *Quality control*

In order to ensure a high-quality dataset, we have employed extensive quality control procedures. The digitized data are scrutinized in four places during the processing, two before and two after filtering. The checking procedures are

- Checks during digitizing. The first check occurs in the digitization program. The technician is asked to verify the header containing all of the housekeeping information that was entered for the trace. The program then performs a check on the length of the episode and the technician verifies the computed totals for length of time and precipitation amount.
- Checks during data transfer. During the data transfer from our data entry computer to the data processing computer, each trace is displayed on a graphics CRT. The housekeeping information is again checked, and the shape of the digitized trace is compared to the original. Traces having errors are marked for deletion at this point.
- Checks against published data. The 1-min rates resulting from the processing program are summed by the hour, printed, and then compared to the amounts published in *Local Climatological Data.*
- Checks on extreme values. The final quality con-

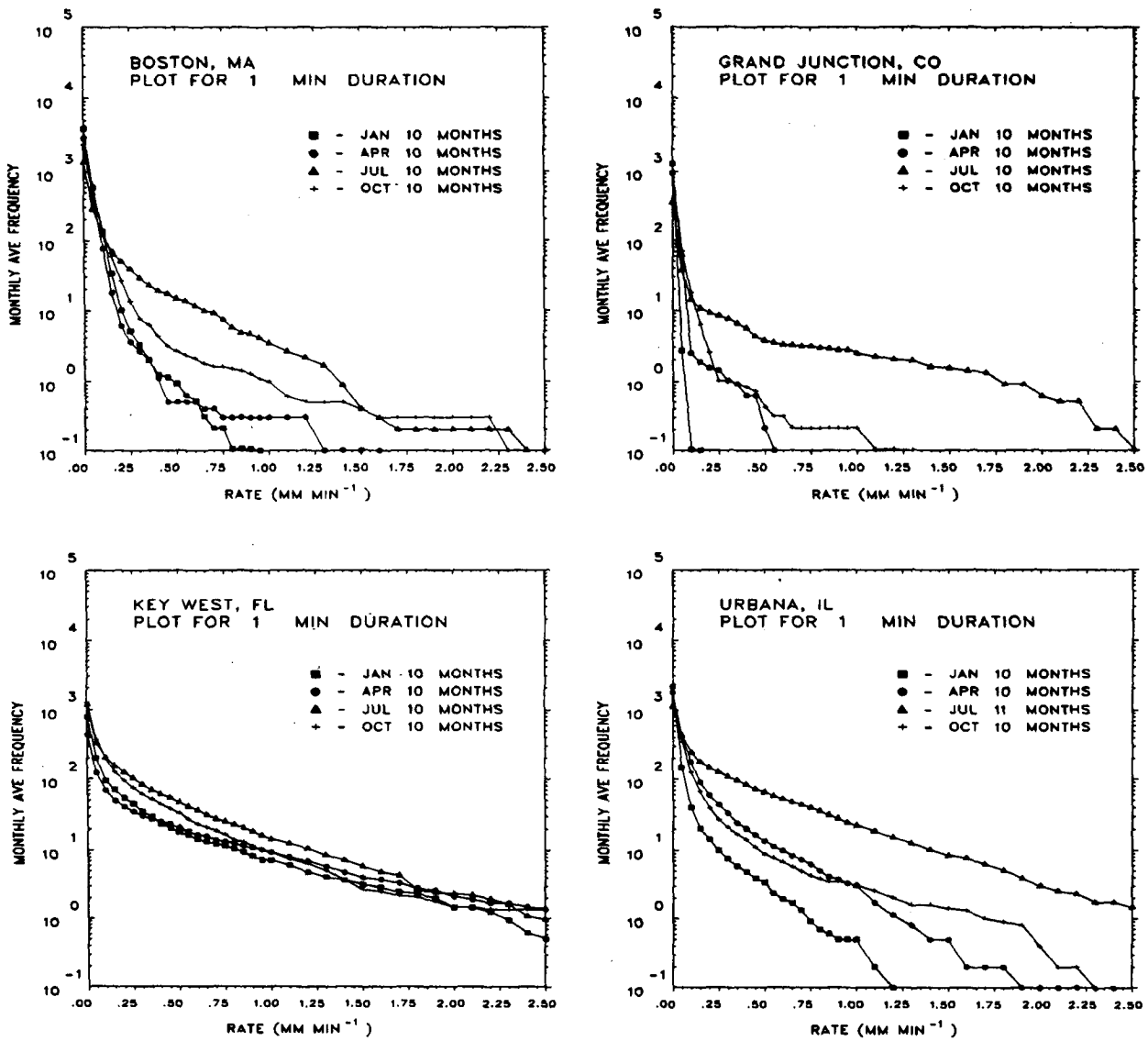

FIG. 6. Average frequency of 1-min rain rates for midseason months at Boston, Grand Junction, Key West and Urbana.

trol step is used to check extreme or possibly anomalous data. An entry in a log file is automatically made if one or more of three criteria are met. The three criteria are 1) high precipitation rate ($\geq$1.25 mm min^{-1}); 2) a large discrepancy in the maximum precipitation rate between filtered and unfiltered data ($\geq$0.5 mm min^{-1}); and 3) excessively short wavelengths used in the reconstruction of the trace after filtering ($\leq$2.5 min).

4. Analyses of 1-min rates

The analyses of 1-min rates presented here are intended primarily to assess the impact of rain on EHF communications. Most previous studies of short-duration rain rates for use in attenuation models provide data in the form of annual rain-rate frequencies (Tattelman and Grantham 1985). Annual statistics can be very misleading, however, because critical rates are concentrated in only a few months of the year at most locations. A low annual frequency of a critical rate can be intolerably high in these months. Although annual rain-rate frequencies are presented, monthly or seasonal rain-rate statistics are preferable for assessing the impact of attenuation caused by rain.

As noted in section 2, a small percentage of the rain data was not available for digitization (see Table 1). Since hourly amounts were available for these periods, it was possible to estimate the percent of the total rain data that was missing at each location. This information was used to adjust the rain-rate analyses by using the following correction factor:

$$\text{correction factor} = \frac{T_{CH}}{T_{CH} - T_M}$$

where T_{CH} is the total number of clock hours of rain and T_M is the number of clock hours of rain that was missing (i.e., not available for digitization). This correction factor is based on the premise that 1-min rain rates during the missing clock hours are distributed the same as the available 1-min data. This is reasonable since missing hours are associated with equipment problems and are not correlated with rain-rate intensity.

a. Rain-rate duration frequencies

Annual average rain-rate frequencies for six duration times are provided for Boston, Denver, Key West, and Urbana in Fig. 4. Rain rates are equaled or exceeded during each minute of the specified duration. Actual frequencies are plotted for every 0.05 mm min^{-1} rate up to 1.00 mm min^{-1} and for every 0.10 mm min^{-1} thereafter. Values plotted for a frequency of 10^{-2} represent the highest rate that was equaled or exceeded for the specified duration.

Monthly average rain-rate frequencies for six different duration times are provided for the worst (most extreme) month at Denver, Omaha, Rapid City, and Seattle in Fig. 5. Values are plotted in the same manner as Fig. 4. The worst month at each location was subjectively chosen from all the monthly plots to (generally) represent the highest frequencies of rates for all durations. Frequencies for some rates and durations may be higher in other months.

To get an appreciation of how the frequency of 1-min rates varies during the year, Fig. 6 provides monthly average frequencies of 1-min rates for midseason months at Boston, Grand Junction, Key West, and Urbana. Frequencies of high rates are generally greatest during July at most locations when heavy convective showers are most common. Variability is least for Key West where rates are relatively high during each of the months.

b. Rain-rate duration probabilities

For many design considerations it is more practical to express the likelihood of events in terms of their

TABLE 2. One-min rainfall rate (mm/min) vs duration and probability of at least one occurrence(s) during the worst month.

		Duration (min)														
		5			10			15			20			30		
		Probability			Probability			Probability			Probability			Probability		
Location	Worst month	0.1	0.5	0.9	0.1	0.5	0.9	0.1	0.5	0.9	0.1	0.5	0.9	0.1	0.5	0.9
Boston	Aug	1.19	0.86	0.48	0.90	0.47	0.26	0.60	0.33	0.16	0.36	0.22	0.13	0.30	0.15	0.09
Denver	Aug	1.49	0.73	0.38	1.18	0.38	0.22	0.64	0.28	0.13	0.44	0.22	0.09	0.29	0.12	0.07
Grand Junction	Jul	1.39	0.37	0.10	0.97	0.10	0.06	0.92	0.08	0.04	0.34	0.06	0.04	0.15	0.04	0.03
Key West	Aug	1.70	1.50	1.03	1.59	1.00	0.59	1.01	0.68	0.40	1.00	0.52	0.24	0.79	0.31	0.10
Omaha	Jul	1.60	1.09	0.68	1.00	0.69	0.39	0.90	0.45	0.24	0.65	0.39	0.15	0.65	0.20	0.09
Rapid City	Jun	1.30	0.77	0.50	0.75	0.49	0.24	0.65	0.29	0.18	0.60	0.20	0.14	0.25	0.16	0.11
Seattle	Sep	0.45	0.26	0.16	0.39	0.17	0.12	0.35	0.13	0.10	0.20	0.12	0.09	0.11	0.09	0.07
Urbana	Jul	1.96	1.38	1.00	1.63	0.87	0.41	0.84	0.51	0.22	0.82	0.28	0.14	0.24	0.11	0.08

TABLE 3. One-minute rainfall rate (mm/min) vs duration and probability of at least three occurrence(s) during the worst month.

		Duration (min)														
		5			10			15			20			30		
		Probability			Probability			Probability			Probability			Probability		
Location	Worst month	0.1	0.5	0.9	0.1	0.5	0.9	0.1	0.5	0.9	0.1	0.5	0.9	0.1	0.5	0.9
Boston	Aug	0.71	0.44	0.33	0.37	0.24	0.17	0.23	0.15	0.12	0.18	0.13	0.09	0.13	0.09	0.06
Denver	Aug	0.53	0.35	0.23	0.32	0.19	0.10	0.22	0.11	0.07	0.14	0.08	0.05	0.09	0.06	0.04
Grand Junction	Jul	0.26	0.09	0.06	0.09	0.05	0.03	0.06	0.04	0.03	0.05	0.03	0.02	0.04	0.02	0.01
Key West	Aug	1.32	1.00	0.75	0.84	0.57	0.37	0.57	0.37	0.19	0.42	0.22	0.13	0.23	0.09	0.06
Omaha	Jul	0.96	0.65	0.44	0.56	0.36	0.20	0.38	0.22	0.11	0.26	0.13	0.08	0.14	0.08	0.05
Rapid City	Jun	0.67	0.46	0.27	0.41	0.22	0.16	0.24	0.17	0.13	0.18	0.13	0.10	0.14	0.10	0.07
Seattle	Sep	0.20	0.15	0.12	0.15	0.12	0.09	0.12	0.09	0.08	0.11	0.09	0.07	0.08	0.07	0.05
Urbana	Jul	1.27	0.91	0.63	0.80	0.38	0.23	0.37	0.20	0.12	0.22	0.13	0.08	0.09	0.07	0.05

probability. The Poisson distribution is an appropriate tool for quantifying random events, such as rainfall occurrences, if the events in any time interval are statistically independent of events in another time interval. In this case, rain events have 5-, 10-, 15-, 20-, and 30-min durations and the time interval is a specified month of the year (e.g., July). Since these rain events are independent from year to year, the probability, P, of y rain events in a month can be calculated using the Poisson formula

$$P(y) = \frac{e^{-\lambda}\lambda^{y}}{y!} \tag{3}$$

where λ is the mean number events per month. Therefore, the probability of *at least* y occurrences of an event is

$$P(\text{at least } y) = 1 - \sum_{z=0}^{y-1} P(z).$$

One-min rainfall rates versus duration and the probability of at least one occurrence during the worst month are provided in Table 2. Rates corresponding to the probability of at least three occurrences during the worst month are provided in Table 3. The worst (most severe) month was subjectively chosen to "generally" represent the highest rates for each probability and duration. Rates for some probabilities and durations may be higher in other months.

Table 4 presents the longest duration at or above specified threshold rain rates and the month of the year that it occurred. Since these are the most extreme occurrences in 10 yr (10.25 yr at Urbana), the probability that they would occur in that month in any one year is approximately 0.1.

c. *Time between events*

To more completely assess the impact of an attenuation outage due to rain, it is also important to know how soon an outage may recur; i.e., if it is raining at or above a critical rate then drops below that rate, what time period would elapse before the rate was exceeded again? We call the period of time between the occurrence of specified rates the time between events (TBE).

TABLE 4. Longest duration (minutes) of 1-min rates (in parentheses) at or above specified threshold rates and the month of occurrence.

	Threshold rate (mm/min)								
Location	0.1	0.2	0.4	0.7	1.0	1.3	1.6	2.0	2.5
Boston	(275) Jan	(52) Sep	(23) Sep	(13) Sep*	(7) Jul†	(7) Jul	(3) Oct	(3) Oct	(1) Oct†
Denver	(162) Jun	(47) Aug	(20) Aug	(13) Aug	(12) Aug	(6) Aug	(4) Aug*	(4) Jul	(3) Jul
Grand Junction	(40) Jul	(24) Jul	(19) Jul	(17) Jul	(10) Jul	(8) Jul	(4) Jul	(2) Jul	(1) Jul
Key West	(156) May	(74) Aug	(61) Apr	(39) Apr*	(22) Aug	(12) Aug*	(10) Aug	(7) Jul*	(4) Jul*
Omaha	(142) May	(67) Jul	(42) Jul	(18) Jul	(12) Jul*	(9) Jul	(5) Jul*	(3) Jul‡	(3) Aug*
Rapid City	(149) Jun	(55) Jun	(28) Jul	(16) Jul	(11) Jul	(8) Jul	(8) Jul	(6) Jul	(4) Jul
Seattle	(82) Feb	(59) Oct	(13) Sep	(2) Aug*	(0) —	(0) —	(0) —	(0) —	(0) —
Urbana	(91) Oct	(45) May	(37) May	(25) Jun	(20) Jun	(14) Jun	(10) Jul*	(5) Jul*	(4) May

* Also occurred in 1 other month.
† Also occurred in 2 other months.
‡ Also occurred in 3 other months.

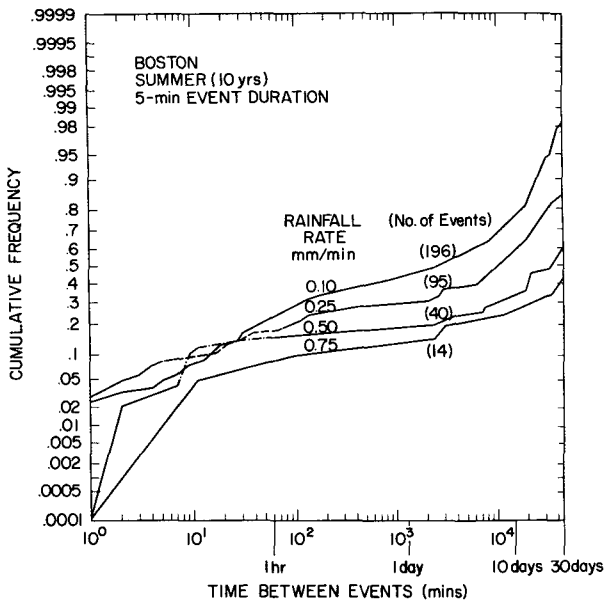

FIG. 7. Cumulative frequency distribution of the time between events categorized by rain intensity at Boston during the summer for a 5-min event duration.

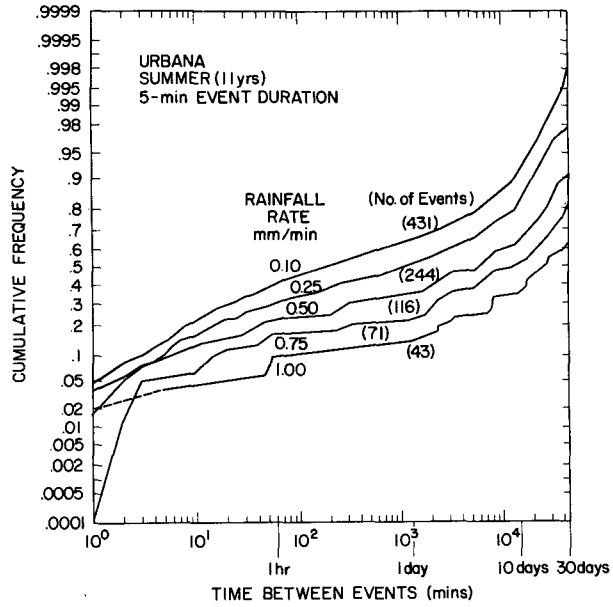

FIG. 9. As in Fig. 7 except for Urbana.

For this study, we considered five threshold rates, 0.10, 0.25, 0.50, 0.75 and 1.00 mm min^{-1}, which were equaled or exceeded for each of 5 (and 10) consecutive minutes. Each rate and duration constitutes an event, for a total of five 5-min events and five 10-min events. When an event occurs (e.g., a rate of at least 0.10 mm min^{-1} for 5 consecutive min), what is the TBE until this event recurs?

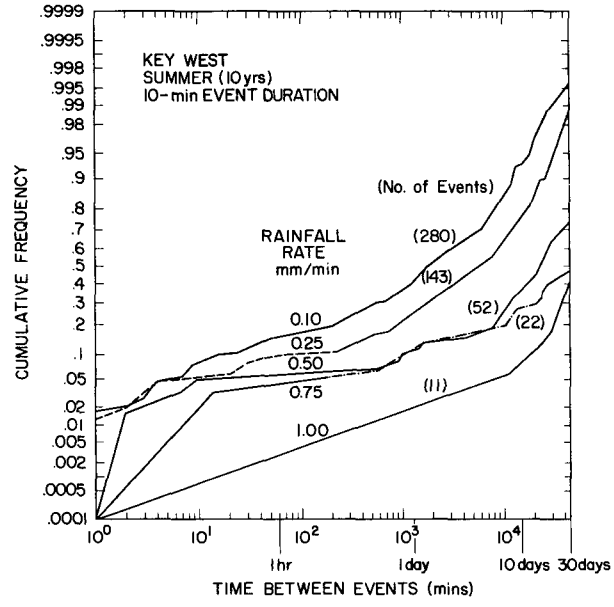

FIG. 8. As in Fig. 7 except for Key West for a 10-min event duration.

The TBEs at each location were determined for each meteorological season (e.g., summer is June, July, and August). The first and last TBE for each season was determined by scanning for 30 days prior to the beginning and after the end of the season. For example, if the first event occurred on 5 June, the first TBE is determined by scanning the last 30 days for a previous event at that threshold rate and duration. If there were no prior event within the scan, the TBE is considered to be greater than 30 days and is lumped with other TBEs greater than 30 days.

Continuing with this example, if there were no other events for the remainder of the summer season, the scan stops on 31 August and a second TBE greater than 30 days is recorded. If, however, a recurrence happened on 30 August, another TBE greater than 30 days is recorded and the scan continues until the next event, or until 29 September, to determine the last TBE. If there are no more events, there are three TBEs, all of which are greater than 30 days. If there are no events during an entire season, a TBE is not tallied. For TBEs up to 30 days, the exact time period is recorded.

The cumulative probability distributions of TBE for Boston, Key West, and Urbana during the season with the greatest number of events (summer) are provided in Figs. 7, 8, and 9. The number of events indicated in the figures are for ten summer seasons at Boston and Key West, and 11 summer seasons at Urbana. Dots and dashes in the figures are used to show continuity of lines where they cross.

5. Summary

One-minute rain rates can be effectively extracted for long periods of time at locations for which weighing raingage recordings are available. The method described employs magnification of original chart records with modern digitizing and filtering techniques to obtain the 1-min data that are ordinarily unreadable.

Analyses of the frequency and duration of 1-min rain rates for a 10-yr period of record is provided for the following eight United States locations: Boston, Denver, Grand Junction, Key West, Omaha, Rapid City, Seattle and Urbana. Particular attention is given to the frequency and probability of 1-min rates with durations of 1, 5, 10, 15, 20, and 30 min. Results show the high variability of the frequency versus duration and rainfall rate for midseason months at most locations. Variability is least for Key West and Seattle where rates are high and low, respectively, during each of the months.

A study of the time between rainfall events is also provided for three locations, Boston, Key West and Urbana. As an example, these results indicate that 15% to 25% of the rain events with a 5-min duration of 0.10 to 0.50 mm min^{-1} intensities during the summer at Boston occurred within 1 h of another such event.

Acknowledgments. The authors express their appreciation to Kathryn Scharr, Kevin Larson, Andy Mazzella and James Willand for their data processing support, to Donald Grantham and Grant Goodge for their helpful suggestions, and to Carolyn Fadden and Helen Connell for typing the manuscript.

REFERENCES

Bloomfield, P., 1976: *Fourier Analysis of Time Series: An Introduction,* John Wiley & Sons, Inc., 258 pp.

Bodtmann, W. F., and C. L. Ruthroff, 1976: The measurement of 1-min rain rates from weighing raingage recordings. *J. Appl. Meteor.,* **15,** 1160–1166.

Engelbrecht, H. H., and G. N. Brancato, 1959: World record one-minute rainfall at Unionville, Maryland. *Mon. Wea. Rev.,* **87,** No. 8, 303–306.

Jones, D. M. A., and W. M. Wendland, 1983: Statistics of Instantaneous Rainfall Rates, Final report for contract F19628-82-K-0012, AFGL-TR-83-0056.

——, and ——, 1984: Some statistics of instantaneous precipitation. *J. Climate Appl. Meteor.,* **23,** 1273–1285.

Ruthroff, C. L., and W. F. Bodtmann, 1976: Computing derivatives from equally spaced data. *J. Appl. Meteor.,* **15,** 1152–1159.

Tattelman, P., and K. G. Scharr, 1983: A model for estimating one-minute rainfall rates. *J. Climate Appl. Meteor.,* **22,** No. 9, 1575–1580.

——, and D. D. Grantham, 1985: A review of models for estimating 1-min rainfall rates for microwave attenuation calculations. *IEEE Trans. Commun.,* **COM-33,** No. 4, 361–372.

——, and P. T. Willis, 1985: Model Vertical Profiles of Extreme Rainfall Rate, Liquid Water Content, and Drop-Size Distribution. AFGL-TR-85-0200, ADA164424, 42 pp.